





LETTER • OPEN ACCESS

Using long short term memory networks to predict daily-averaged sea level anomaly and surface currents

To cite this article: C R Athul et al 2025 Environ. Res. Lett. 20 104031

View the article online for updates and enhancements.

You may also like

- Intersectional inequalities in heat-related mortality risks in South Korea Sera Kim and Jong-Tae Lee
- Tree mortality provides early warning sign of ecosystem functional transition in coastal freshwater forested wetlands M Aguilos, G Sun, J Bulluck et al.
- Are EVs cleaner than we think? Evaluating consequential greenhouse gas emissions from EV charging Riti Bhandarkar, Qian Luo, Emil Dimanchev et al.



ENVIRONMENTAL RESEARCH

LETTERS



OPEN ACCESS

RECEIVED

17 April 2025

REVISED

12 August 2025

ACCEPTED FOR PUBLICATION 29 August 2025

PUBLISHED

11 September 2025

Original content from this work may be used under the terms of the Creative Commons Attribution 4.0 licence.

Any further distribution of this work must maintain attribution to the author(s) and the title of the work, journal citation and DOI.



LETTER

Using long short term memory networks to predict daily-averaged sea level anomaly and surface currents

C R Athul^{1,2}, B Balaji^{1,3,*}, Vinod Daiya¹ and Arya Paul^{1,*}

- Indian National Centre for Ocean Information Services (INCOIS), Ministry of Earth Science (MoES), Hyderabad, India
- ² KUFOS-INCOIS Joint Research Centre, Faculty of Ocean Science and Technology, Kerala University of Fisheries and Ocean Studies, Kochi, India
 - Indian Institute of Tropical Meteorology (IITM), Ministry of Earth Science (MoES), Pune, India
- * Authors to whom any correspondence should be addressed.

E-mail: balaji.b@incois.gov.in and aryapaul@incois.gov.in

Keywords: sea level prediction, machine learning, neural networks, LSTM

Supplementary material for this article is available online

Abstract

Short-term prediction of sea level anomaly (SLA) and ocean surface currents over a domain are usually carried out using ocean general circulation models. In this study, we present a univariate machine learning framework using long short term memory networks that forecasts daily-averaged SLA with a 3 d lead time over the north Indian Ocean using historical satellite altimetry data at a spatial resolution of \sim 13 km. Assuming that SLA reanalysis from state-of-the-art systems represent the pinnacle of performance skill of forecasts from dynamical models, we show that the SLA forecasts from our model exhibits superior skills through comprehensive analyses. The errors are typically less than 0.04 m over most of the domain and the correlations are close to unity. The skills of the daily-averaged forecasted currents with a 3 d lead, estimated using geostrophic and Ekman theory, are comparable with the best available reanalysis when compared to *in-situ* observations both in the open ocean or shelf. Treating these forecasted surface currents as synthetic observations, we show that assimilating them can significantly improve the instantaneous subsurface currents during forecasts. The subsurface correlations turn significant with 99% confidence level across depth which were otherwise mostly insignificant and the errors reduce by $0.1 \text{ m} \cdot \text{s}^{-1}$. We demonstrate that the short-term forecast of daily-averaged SLA and surface currents can be approached as a collection of localized low-dimensional independent univariate systems thereby reducing computational costs by large margins. This machine learning framework heralds a paradigm shift in the realm of ocean forecasting.

1. Introduction

Early knowledge of sea level anomaly (SLA) and ocean surface currents aids coastal zone management, harbor operations, and offshore marine industries. Accurate forecasts of ocean surface currents assist disaster management involving marine debris and lost persons/objects in the sea, influence ocean ecosystems at the euphotic zone (Garçon *et al* 2001), and act as an early predictor of marine animal behavior (Chapman *et al* 2011). These forecasts have been conventionally carried out using ocean general circulation models, which solve dynamic equations but suffer from unreliability stemming from inaccurate initial conditions,

approximations in model physics, errors in atmospheric fluxes, etc. Consequently, the forecasts are compromised even though observations from various platforms are regularly assimilated into the model to arrest errors from compounding.

Recent years have seen an abundance of research endeavors that have used diverse machine learning (ML) techniques ranging from regression methods to various types of neural networks to model sea levels at *in-situ* locations or over a small area (Nikoo *et al* 2018, Guillou and Chapalain 2021, Tur *et al* 2021, Kartal and Altunkaynak 2024, Shola *et al* 2024). The ML methods stand out for their ability to learn the physical processes involved in the dynamics of

a predictor-predictand relationship, offering a selfadaptive, data-driven approach to model the predictand. However, successful short-term forecasting of SLA using univariate ML models wherein only SLA or some derivative of it serves as both the predictor and predictand (Kartal and Altunkaynak 2024) is surprising and challenges our perception of the SLA dynamics. This is due to the lack of other variables in the predictor (e.g. winds, air pressure, etc), since the temporal evolution of SLA is dynamically influenced by atmospheric forces and other ocean state variables such as ocean currents, temperature, and salinity (Pedlosky 2013, Gill 2016). This astonishment is further compounded when in-situ SLA is faithfully predicted through ML using only collocated historical SLA observations (Kartal and Altunkaynak 2024) because SLA is known to be remotely influenced even by waves generated thousands of kilometers away (Rohith et al 2019, Afroosa et al 2021). This study suggests that a complex system like an ocean, where an ocean state variable at any location is dynamically coupled to all state variables across locations, may be approximated as a set of simple, separate systems that operate independently in specific regions. In this approach, the SLA at any location can be individually trained using only historical SLA data at that location and modeled through ML.

However, our attempt to predict daily-averaged SLA over the north Indian Ocean (NIO) using satellite altimetry via the same formalism (Kartal and Altunkaynak 2024) involving K-nearest neighbors (Fix and Hodges 1952) and empirical mode decomposition (Huang et al 1998) is met with phase lags in the predictions exceeding the prediction horizon by several days thereby rendering the framework ineffective. There are however other ML frameworks that can potentially do the job. For example, long short-term memory (LSTM) networks (Hochreiter and Schmidhuber 1997), a type of recurrent neural network (RNN), have gained significant attention for their ability to model sequential data and capture long-term dependencies and have emerged as powerful tools for time series prediction in the marine sciences. Several studies have explored the application of LSTM models to predict SLA, demonstrating their effectiveness compared to traditional statistical and other ML methods. Accarino et al (2021) presented a ML approach using LSTM to predict short-term sea levels at various coastal stations in the Southern Adriatic Northern Ionian region of the Mediterranean Sea and demonstrated that the LSTM model could forecast mean sea levels three days in advance with higher accuracy than the dynamical model SHYFEM (Umgiesser et al 2004, Federico et al 2017). LSTM Auto-Encoders has also been shown to improve SLA predictions over Black Sea with a 3 d lead time (Yavuzdoğan and Kayıkçı 2025). Jorges et al (2021) developed and compared ML models to reconstruct and predict near shore significant wave heights with a novel method of integrating bathymetric data. LSTM came out as the best-performing model compared to traditional ML models, with bathymetry further improving the accuracy.

Winona and Adytia (2020) used a deep learning approach with LSTM to forecast sea level at a tide gauge location near Bali using 2 months of training data and found that the LSTM with feedback achieved outstanding performance (Correlation (R) = 0.999, root mean squared error (RMSE) = 0.019-0.028) for forecasts from 7 d to 60 d, outperforming the nofeedback LSTM and tidal harmonic analysis. Balogun and Adebisi (2021) used autoregressive integrated moving average (ARIMA), support vector regression, and LSTM models to predict sea level variation along the West Peninsular Malaysia coastline using combinations of ocean and atmospheric variables, and found that LSTM with combined inputs performed best (mean R = 0.853), except at one location where ARIMA excelled, highlighting the importance of region-specific dominant physical processes. Chen et al (2023) developed a hybrid VMD-EEMD-LSTM (Variational Mode Decomposition and Ensemble Empirical Mode Decomposition) model to predict sea level near the Dutch coast and found it significantly outperformed individual and other hybrid models, achieving RMSE = 47.2 mm, mean absolute error (MAE) = 33.3 mm, and R^2 = 0.9, with improvements up to 58.7% in root mean squared error (RMSE) and 49.9% in R^2 over VMD-LSTM. In short, LSTM models have been extensively used across different regions for SLA predictions. Žust et al (2021) developed high-performance deep tidal residual estimation method using atmospheric data, a deep-learning-based ensemble model for forecasting sea level in the northern Adriatic using European Centre for Medium-Range Weather Forecasts atmospheric and sea level data, which, with a 72 h lead time, outperformed the operational NEMO ocean model by achieving lower RMSEs (10.8 cm overall; 20.2 cm during storm surges) while drastically reducing computational costs, thereby demonstrating its potential for operational coastal flood forecasting.

The success of LSTM in predicting SLA across different basins encourages us to ask the following question: using LSTM, is it possible to forecast shortterm (up to few days) daily-averaged SLA over the domain of NIO using only satellite altimetry data that has been available since 1993? This strategy additionally promises the possibility of short-term prediction of daily-averaged low-frequency surface currents which is broadly a combination of geostrophic and Ekman components (Sudre et al 2013). The geostrophic (Ekman) component of the surface current can be estimated from the forecasted SLA (forecasted winds). This diagnostic mechanism involves no integration over time (local acceleration ignored) and hence is realistic at only low frequencies. The veracity of such surface current predictions however, remains

to be tested since this simplistic formalism of surface current estimation neglects the contributions arising from ageostrophic currents including local acceleration, the Stommel shear dynamics, and surface buoyancy gradients (Dohan 2021).

2. Methods

LSTM (Hochreiter and Schmidhuber 1997) networks are specialized RNNs designed to capture long-term dependencies in sequential data. Traditional RNNs are often hindered by the vanishing gradient problem, making it difficult to retain information over extended sequences (Hewamalage et al 2021). LSTMs mitigate this limitation by using memory cells and gating mechanisms comprising input, forget, and output gates that dynamically control and optimize information flow by selectively retaining or discarding past information, thereby enhancing their capacity to capture and utilize long-range temporal dependencies effectively. Furthermore, LSTM networks employ a multiplicative forget layer with learnable parameters to manage memory more efficiently, enabling the model to determine the relevance of the information (Accarino et al 2021).

Distinct univariate LSTM models are developed target Archiving Validation for Interpretation of Satellite Oceanographic (AVISO) grid point over NIO (5°N-30°N; 45°E-100°E) with an objective to predict daily-averaged SLA with a 7 d lead at a spatial resolution of \sim 13 km. For each target grid point, we consider the daily-averaged altimetry SLA over a 3×3 grid centered around the target grid point with a 2 d lookback period. Consequently, the input length consists of 18 values for every forecast of each target grid. The total period of consideration is 2011-2020 with 2011-2018 as training period and 2019–2020 as the testing period. This results in input features with a shape of (2916, 18) and output features with a shape of (2916, 1) for every target grid point in the NIO during the training period. Both the input and output features were randomized over the first axis (keeping track of indices) to disrupt temporal continuity. The same training process is repeated for every target grid over NIO (44865 grid points excluding land). The prediction after the training suffered from lags ranging from 2–6 d across all grids, with the median lag estimated to be 4 d observed in approximately 65% of the domain (see supplementary figure S1). The issue of phase lags is not an isolated problem but has been acknowledged in many past studies (Pölz et al 2024, Zhang et al 2024). It is also recognized that these lags can be mitigated, to some extent, by randomizing the input sequences—a strategy we have employed in our study. We apply the same randomization technique to the input features of shape (725, 18) during the testing period and use the model to forecast over the 2 year testing period. Thereafter, the predictions during the testing period are lag adjusted

by 4 d effectively transforming them into 3 d forecasts. All the LSTM models used were constructed using the TensorFlow Python package (Dean and Monga 2015). The performance of the LSTM model for various lead times is presented in supplementary figure S2.

The model architecture consisted of two stacked LSTM layers, each with 50 units and ReLU activation, each followed by dropout layers with dropout rate = 0.2 to mitigate over fitting. The output from the second LSTM layer was fed into a dense layer with 25 units and ReLU activation, followed by a final dense layer with a single output neuron for regression. The network was trained using the Adam optimizer with a learning rate of 0.001, and MSE was employed as the loss function. Training was performed for 50 epochs with a batch size of 32.

We emphasize that the LSTM models are oblivious of the testing dataset during the training phase thereby obliterating issues arising from data leakage. Henceforth, all variables are daily-averaged and LSTM-SLA represents predicted SLA from LSTM with a lead of 3 d unless mentioned otherwise.

To evaluate the performance of the LSTM-based SLA predictions, the model outputs are validated against AVISO altimetry observations and compared with the high-resolution (~9 km) global ocean physics reanalysis GLORYS12v1 (henceforth GLORYS) product (Bonjean and Lagerloef 2002), which is perhaps the best available ocean reanalysis (Castillo-Trujillo et al 2023). GLORYS assimilates SLA among other observations (see supplementary information for more details). The 3 d forecasted SLA fields are used to compute geostrophic currents, while Ekman currents are derived using 3 d wind forecasts from (National Centre for Medium Range Weather Forecasting, Prasad et al 2014), which together yield the total surface current estimates. These predicted currents, alongside GLORYS surface currents, are validated against the ocean surface current analysis realtime (OSCAR; Dohan 2021) dataset. Additionally, for validation against in-situ observations, dailyaveraged surface currents from twelve ocean moored buoy network for NIO (OMNI) mooring buoys distributed across the NIO and from an HF-RADAR system deployed along the Tamil Nadu coast are used.

3. Results

3.1. SLA

Assuming that GLORYS represents the asymptotic upper bound of the forecast skill from dynamical models, the performance of LSTM-SLA is compared against the performance of GLORYS-SLA for the period 2019–2020. Consequently, if the LSTM manages to outclass this reanalysis it shall outperform forecasts from dynamical models as well. Both the models are compared against gridded level 4 SLA

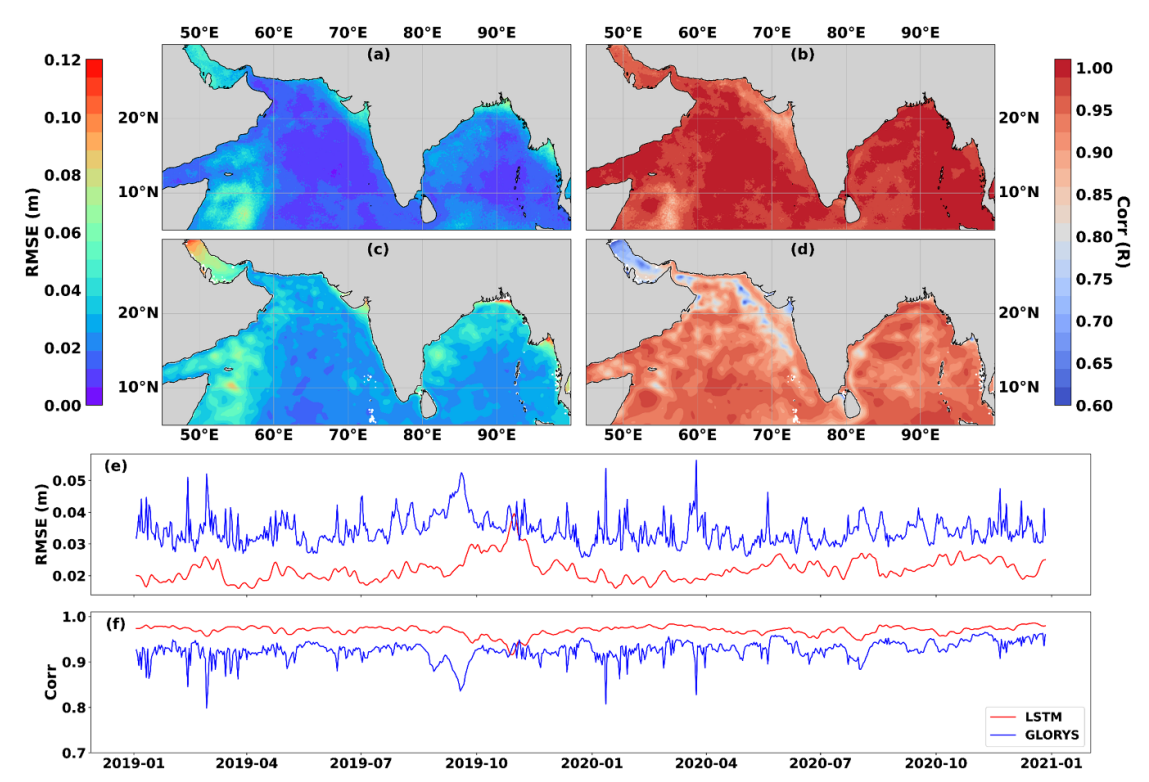


Figure 1. SLA skill comparison of LSTM and GLORYS. RMSE in SLA (in meters) from (a) LSTM and (c) GLORYS with respect to altimetry SLA for the period 2019–2020. The RMSE color bar is on the left. Correlation in SLA from (b) LSTM and (d) GLORYS with respect to altimetry SLA for the period 2019–2020. The correlation color bar is on the right. Correlation values larger than 0.074 are more than 95% significant. Domain-averaged time series of (e) RMSE and (f) correlation coefficient in SLA from LSTM (red) and GLORYS (blue) with respect to SLA from AVISO.

 $(0.125^{\circ} \times 0.125^{\circ})$ from AVISO altimetry. It is important to note that the gridded AVISO-SLA is derived through optimal interpolation of multiple satellite track measurements and is therefore not always actual observation (see supplementary information for more details). The long term mean at each location is subtracted from AVISO and GLORYS before comparison.

Figure 1 displays the RMSE and Pearson correlation coefficients from two models-LSTM-SLA and GLORYS-SLA-across NIO. The RMSE in LSTM-SLA is \sim 2–4 cm across most of the domain except at some isolated patches in the western Arabian Sea and the northwestern Bay of Bengal, where the RMSE reaches up to \sim 7 cm (figure 1(a)). In contrast, the RMSE in GLORYS-SLA (figure 1(c)) is larger by 3-4 cm across the domain. The LSTM-SLA exhibits over 90% correlation with the satellite altimetry (figure 1(b)), indicating the strong skill of the LSTM model in accurately forecasting the phase of the observations. In comparison, the correlations derived from GLORYS (figure 1(d)) also demonstrate strong associations, but certain regions near the northeastern Arabian Sea exhibiting lesser correlations of \sim 70%. The time series of domain-averaged RMSE in LSTM-SLA remains below 4 cm across the period of our study. The GLORYS RMSE, on the other hand, is about twice larger (see figure 1(e)). The domain-averaged correlation coefficient in the

LSTM remains close to unity across the entire period (see figure 1(f)). GLORYS exhibits relatively weaker correlation (\sim 0.9), indicating its limitations in reproducing the phases of the SLA correctly. Although the dynamical model GLORYS demonstrates a good skill in terms of phase alignment with observations, it is important to emphasize that the LSTM outperforms GLORYS by achieving higher accuracy in forecasting SLA over the NIO three days in advance. This is surprising given that a forecasted SLA with a lead time of 3 d outclasses one of the best state-of-the-art SLA reanalysis which is generated in hindcast.

Traditional evaluation metrics, such as correlation and RMSE, provide useful insights into forecast accuracy and skill by focusing on overall agreement, linear dependence, and error magnitude (Murphy 1993). However, probability distributions like marginal, joint and conditional distributions, which contains all time independent information relevant to evaluating forecast quality and probability-based metrics, such as Kullback-Leibler divergence (KL, Kullback and Leibler 1951) and mutual information (Thomas et al 2005), offer a more comprehensive evaluation by considering the entire distribution of modeled and observed values. The KL divergence between LSTM and AVISO SLA is 0.0266, whereas for GLORYS, it is 1.8751—larger by two orders of magnitude—suggesting that LSTM provides a more

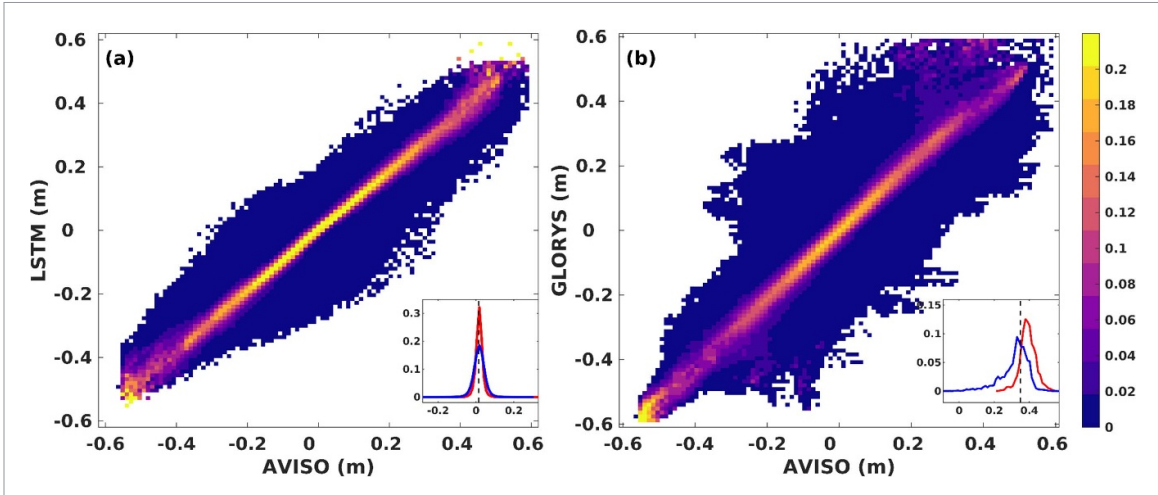


Figure 2. Conditional probability distributions. (a) Conditional probability distribution of observations (AVISO SLA) given LSTM-SLA. (b) Conditional probability distribution of observations (AVISO SLA) given GLORYS-SLA. The inset of figure(a) represents the conditional probability of AVISO SLA at a given SLA = 0.015 m from LSTM (red) and from GLORYS (blue). The dashed vertical line is at 0.015 m. Similarly, the inset of figure(b) shows the conditional probability of AVISO SLA at a given SLA = 0.33 m from LSTM (red) and from GLORYS (blue). The dashed vertical line is at 0.33 m.

accurate probabilistic representation. Additionally, we computed symmetric uncertainty (SU; Witten et al 2005), a normalized version of mutual information, which quantifies how much information the forecast retains about the observations. A higher SU indicates better predictive skill. The SU measure between LSTM and observations is 0.4488, compared to 0.3044 for GLORYS, further supporting that LSTM provides better predictive performance. The comparison of joint probability density of AVISO SLA and LSTM-SLA with that of AVISO SLA and GLORYS-SLA during 2019–2020 attests to these findings (see supplementary figure S3). Overall, these probabilitybased evaluations confirm that although both models reflect important features of the observed SLA, LSTM shows better accuracy in its predictions. Notably, the 3 d lead SLA forecast from the LSTM model outperforms GLORYS SLA reanalysis.

Reliability (Murphy 1993) is another key aspect of forecast evaluation that measures how well the forecast eventually agrees with actual observations. To evaluate how reliable the models are, we plot the conditional probability distribution of AVISO SLA based on LSTM-SLA (figure 2(a)) and GLORYS-SLA (figure 2(b)). In both plots, the densest areas fall along the diagonal, showing a strong match between predictions and real observations. However, there are clear differences in their probability patterns. The LSTM model shows a tighter, more focused pattern along the diagonal, meaning it predicts SLA more accurately and with less spread. On the other hand, GLORYS has a wider distribution, especially at higher SLA values, which suggests more uncertainty. The inset plots help highlight these differences further. When either LSTM or GLORYS predicts an SLA of 0.015 m, the observed SLA tends to align closely with this predicted value (see inset of figure 2(a)). Notably, 96% of the time, the observation lies within the predicted LSTM

SLA of 0.015 ± 0.04 m. In contrast, GLORYS achieves an accuracy rate of 87%. However, the accuracy of LSTM (GLORYS) decreases to 67% (50%) when it predicts (estimates) a larger SLA = 0.33 m. This is illustrated in the inset of figure 2(b). These findings suggest that LSTM provides very reliable forecasts possibly unmatched by any dynamical models.

3.2. Surface currents

The remarkable fidelity of the forecasted SLA over NIO promises an avenue to forecast daily-averaged ocean surface currents, which can be approximated as a sum of geostrophic and Ekman components. In this study, the surface geostrophic currents in the LSTM framework are computed from the forecasted SLA while the Ekman currents are estimated from the forecasted winds (see supplementary information for details). The forecasted surface currents, therefore, neglect contributions from Stommel shear dynamics, surface buoyancy gradients etc. In contrast, GLORYS provides dynamically obtained hindcasted surface currents estimates, i.e. it includes all known contributions in addition to the assimilation of various observations including SLA. In the absence of any basin-scale surface current observations, surface currents from these two systems—LSTM and GLORYS are compared to daily data from the OSCAR nearsurface (top 30 m averaged) currents. The GLORYS currents are also averaged over the top 30 m.

Both the zonal and meridional predicted surface currents from LSTM with a lead of 3 d show smaller RMSE and larger correlations with respect to corresponding OSCAR currents in comparison to surface currents from GLORYS (see supplementary figures S4 and S5). Surprisingly, the performance of the forecasted surface current in the LSTM estimated from suboptimal 3rd day forecasted winds is better than the GLORYS reanalysis derived from optimal winds.

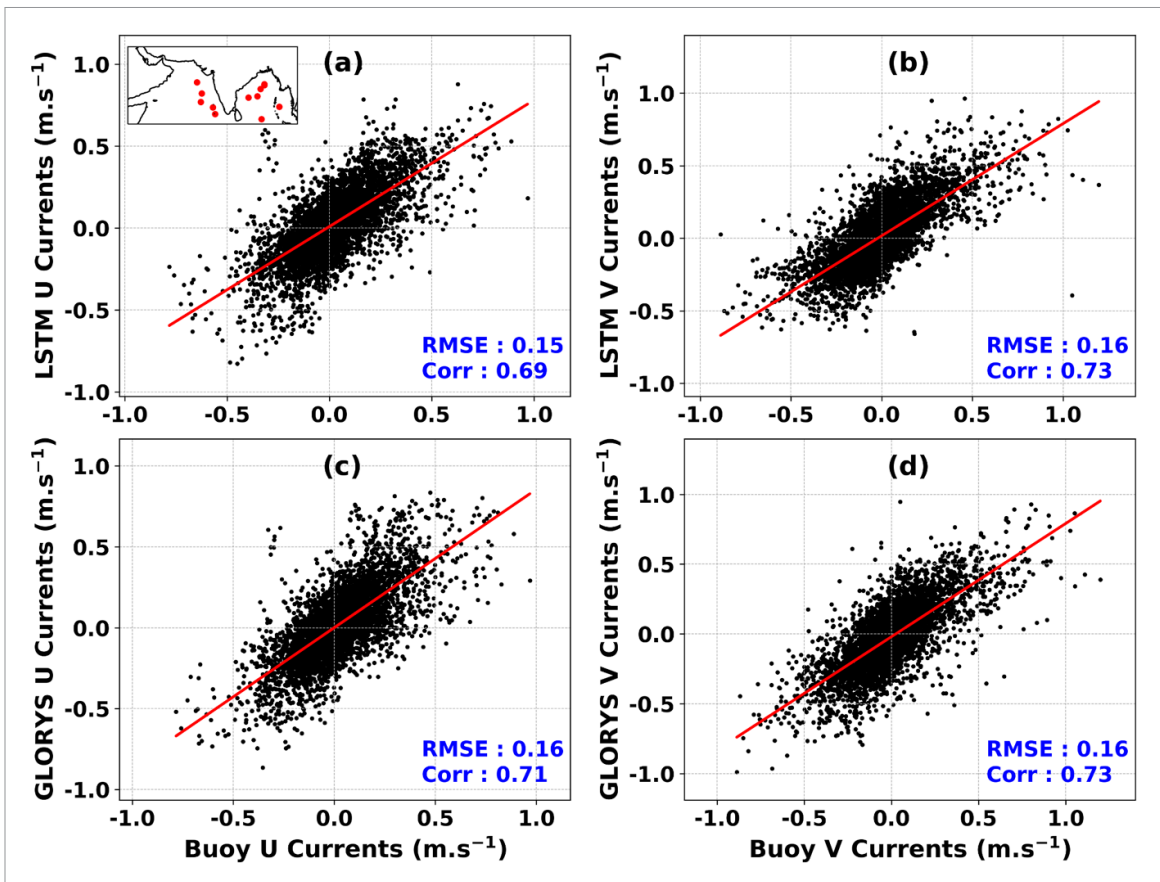


Figure 3. Skill comparison of surface currents from the LSTM and GLORYS. Scatter plots comparison of the time series of zonal currents from (a) LSTM and (c) GLORYS with zonal currents from 12 OMNI buoys. Scatter plots comparison of the time series of meridional currents from (b) LSTM and (d) GLORYS with meridional currents from 12 OMNI buoys. The *x*-axis (*y*-axis) represents the buoy (model) current. RMSE (in $m \cdot s^{-1}$) and correlation indices are shown in the bottom right of each panel. All correlation values are >95% significant. The location of the buoys are marked in the inset plot of (a).

This is possibly because the geostrophic surface currents (derived from SLA) dominate the Ekman surface currents (derived from winds) in the NIO across all seasons of a year (see supplementary figure S6). This analysis also indicates that the key to improving surface currents in the NIO may lie in the improved reproduction of SLA in the dynamical models.

Comparison with OSCAR is only indicative and not a true reflection of the skills of the two models because of two reasons—(1) OSCAR currents are not actual observations, (2) ocean currents shows strong variability along depth in NIO (see figure 5(b) in Venkatesan *et al* 2013) which is captured in OSCAR and GLORYS (top 30 m averaged) but not in LSTM. Therefore we evaluate LSTM and GLORYS surface currents against daily-averaged surface currents from 12 *in-situ* OMNI buoys (Venkatesan *et al* 2013) (see supplementary table 1 for more details) spread across the NIO that measure surface currents every hour with a resolution of 1 cm \cdot s⁻¹ and accuracy of 5 mm \cdot s⁻¹.

Figure 3 shows scatter plots of the zonal and meridional currents from 12 OMNI buoys with zonal and meridional currents from the LSTM model (figures 4(a) and (b)) and GLORYS (figures 4(c) and (d)). The forecasted currents from LSTM and the surface current reanalysis from GLORYS show a

reasonably good agreement with the buoy currents with low RMSE (\sim 0.16 m · s⁻¹) and strong correlations exceeding 0.7. The skills of these two systems in simulating surface currents appear comparable. These results demonstrate the ability of the LSTM model to forecast surface currents with fidelity across the domain with skills similar to GLORYS but with a lead time of 3 d.

The performance of this ML framework is also tested close to the coast with respect to HF-RADAR that measures surface currents every 6 km up to 200 km from the coast and thereafter compared against GLORYS. The distribution of errors in zonal and meridional currents from these two models show that the errors in LSTM is comparable to that of GLORYS (see supplementary figure S7). The RMSE is similar in both the models across the directions but GLORYS exhibits marginally better correlations. The similar spread of the interquartile range in LSTM and GLORYS indicates that most of the model departures are equally spread around zero. The long (short) tails in the error distribution of meridional (zonal) currents in both LSTM and GLORYS demonstrates that there are large departures in modeling the meridional components, in agreement with previous findings (Lellouche et al 2021). It shows that the surface coastal currents predicted by LSTM are comparable with the

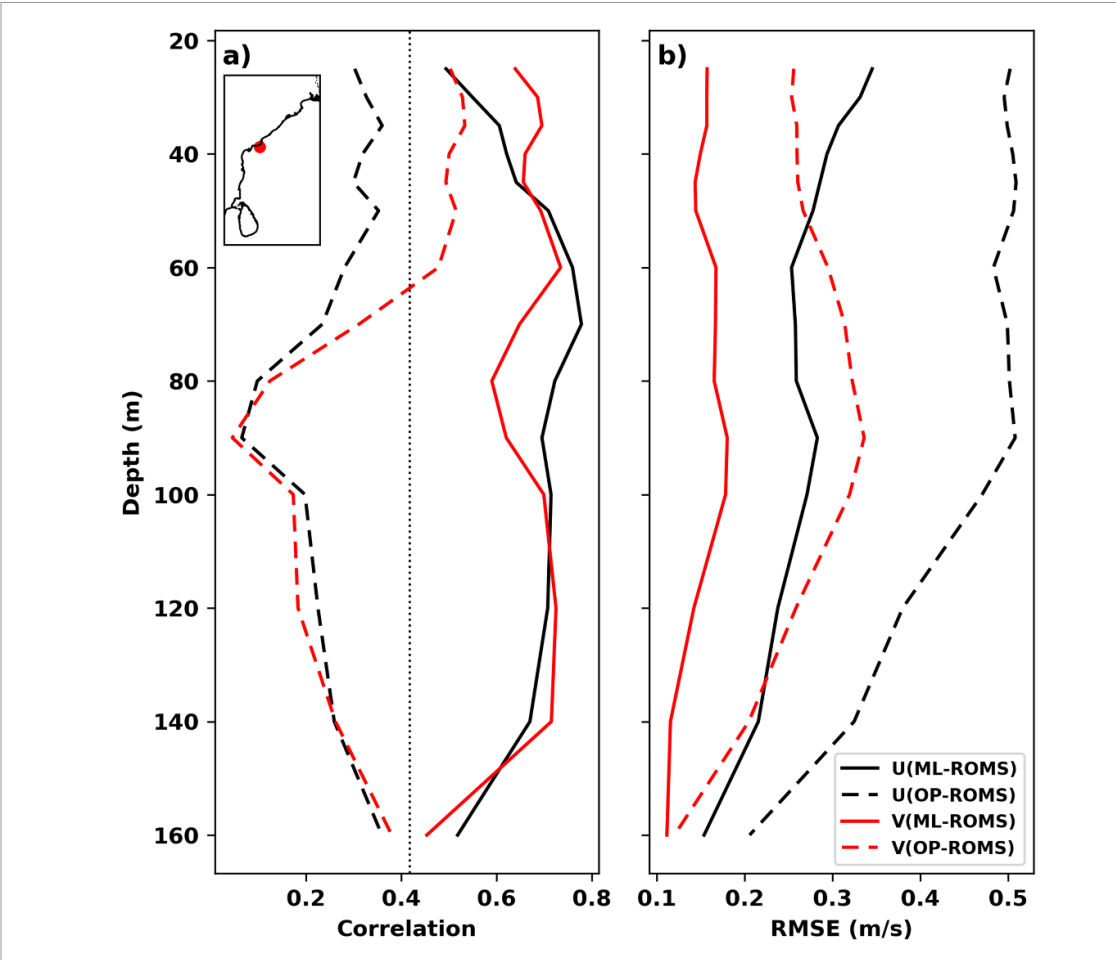


Figure 4. (a) Pearson correlation coefficient of zonal (black) and meridional (red) currents from ML-ROMS (solid) and OP-ROMS (dashed) with respect to ADCP measurements for the period January–June 2020. The vertical dotted line in black at 0.418 represents the threshold correlation coefficient for 99% confidence level. (b) RMSE (in $m \cdot s^{-1}$) of zonal (black) and meridional (red) currents from ML-ROMS (solid) and OP-ROMS (dashed) with respect to ADCP measurements for the same period.

surface coastal current reanalyses generated by the dynamical model GLORYS. In short, LSTM predicts GLORYS-like surface currents both in open ocean and near-shore but 3 d ahead of time.

The accuracy of the forecasted SLA and surface currents raise the possibility of treating it as 'synthetic' observations and assimilate it during the ocean forecast. This assimilation is likely to improve the subsurface features as well. For example, we treat the 3rd day predicted surface currents as synthetic observations and assimilate it in the ROMS model during ocean forecast (call it ML-ROMS). ML-ROMS do not assimilate any other observations. And compare its instantaneous sub-surface currents against the analysis from a running operational model based on ROMS (OP-ROMS) that assimilates SLA, SST, temperature and salinity using LETKF (Baduru et al 2019, Francis et al 2020) every 5 d during Jan–June, 2020. Both these systems are otherwise identical. We compare the instantaneous currents at t = 00 UTC of every 5th day from these two systems against t = 00UTC currents measured by an ADCP stationed at 85.8°E, 19.4°N off the east coast of India (figure 4).

The RMSE of the zonal (meridional) current at 25 m improves by $\sim 0.15 \text{ m} \cdot \text{s}^{-1} \ (\sim 0.1 \text{ m} \cdot \text{s}^{-1})$. This is significant given that the standard deviation in observed zonal (meridional) currents at 25 m is $0.4 \text{ m} \cdot \text{s}^{-1} (\sim 0.2 \text{ m} \cdot \text{s}^{-1})$. Significant improvements are observed even beyond the mean climatological thermocline depth of 72 m estimated from World Ocean Atlas monthly climatology. A strong improvement in correlation is observed with most prominent improvements at 60-120 m. Interestingly, the correlations in zonal and meridional currents from ML-ROMS remains significant at the 99% confidence level across depth while only the meridional current remains significant in OP-ROMS in the top 60 m. This case study underscores the importance of these synthetic observations, which promise substantial enhancements in ocean state forecasts, offering significant benefits to various stakeholders. The readers should however be mindful that these 'synthetic' observations do not include the ageostrophic components. Consequently, the veracity of this framework is likely to suffer in regions where ageostrophic components are significant.

4. Conclusion and discussion

This study introduces a novel methodology of generating realistic daily-averaged SLA and surface currents with a lead time of 3 d using a univariate ML framework. The 3rd day forecasted SLA over NIO follows the altimetry data with striking accuracy and is superior to GLORYS-SLA reanalysis. The forecasted ocean surface currents with a 3 d lead time show a close correspondence with the surface currents from gridded OSCAR analysis, *in-situ* open ocean OMNI buoys and coastal currents from HF-RADAR. Needless to mention, this entire framework can be easily extended to the global domain with suitable adjustments on the estimation of geostrophic currents in the equatorial belt (Sudre *et al* 2013, Dohan 2021).

The success of this univariate approach highlights an important insight: SLA prediction at a given location—or across a region—can be achieved using only historical SLA data from neighboring areas. This is counterintuitive, considering that the dynamical theory of SLA evolution (Pedlosky 2013) involves complex interactions between oceanic and atmospheric state variables. Moreover, SLA is known to be remotely influenced by wave activity originating thousands of kilometers away (Rohith et al 2019), as well as by local bathymetry. Nevertheless, the efficacy of this simplistic counterintuitive SLA prediction framework and the subsequent derivation of surface currents raises hope about the possibility of similar frameworks for other ocean state variables. The veracity of these predictions opens up the possibility of using these as synthetic observations and assimilating them in dynamical models during forecasts when no actual observations are available. Such a mechanism shall help to propagate surface information downwards improving the sub-surface features during forecasts leading to a holistic improvement in the three-dimensional ocean state prediction.

The application of ML models in sea level prediction, while very promising, comes with limitations (Lou *et al* 2023). Since the effectiveness of these models rely extensively on historical data, extracting meaningful information beyond the conditions enshrined in the training datasets remains challenging. The quality, quantity and spatio-temporal resolution of training datasets determine some of the limitations of the prediction system. Moreover, the stochastic nature of climate systems and their complex interactions with other environmental factors make it difficult for these models to capture and predict the full range of variability in sea levels, especially during cyclones, storm surges, etc (Qin *et al* 2023).

Data availability statement

The SLA and mean dynamic topography from AVISO is freely available at https://data.marine.copernicus.e u/product/SEALEVEL_GLO_PHY_L4_MY_008_047.

The GLORYS12V1 SLA and currents are available at https://data.marine.copernicus.eu/product/ GLOBAL_MULTIYEAR_PHY_001_030/services. The OSCAR currents are available at https://podaac. jpl.nasa.gov/dataset/OSCAR_L4_OC_FINAL_V2. 0. World Ocean Atlas (WOA) temperature data is available at Asia-Pacific Data Research Centre (https://apdrc.soest.hawaii.edu/data/). ADCP current data, Buoy current data (https://incois.gov.in/ portal/datainfo/mb.jsp) and HF-RADAR current (https://incois.gov.in/portal/datainfo/hfradar. jsp) is available upon request. The predicted SLA, surface currents, and subsurface currents from the OP-ROMS model and ML-ROMS model are available at the following link (https://doi.org/10.5281/ zenodo.15099558).

The data that support the findings of this study are openly available at the following URL/DOI: https://doi.org/10.528 1/zenodo.15099558.

Acknowledgment

The authors are grateful to INCOIS and Ministry of Earth Sciences (MoES) for providing essential facilities. ACR extends gratitude to INCOIS and MoES for providing the Research Fellowship support. The authors appreciate Venkat Shesu R for sharing the OMNI Mooring Buoy, ADCP and HF-RADAR data. The writing of some portions of the manuscript has been improved using ChatGPT. This is INCOIS contribution number 587.

ORCID iDs

C R Athul © 0009-0003-3318-3122 B Balaji © 0000-0001-9641-4109 Vinod Daiya © 0009-0002-1870-0374 Arya Paul © 0000-0002-6635-3058

References

Accarino G, Chiarelli M, Fiore S, Federico I, Causio S, Coppini G and Aloisio G 2021 A multi-model architecture based on long short-term memory neural networks for multi-step sea level forecasting *Future Gener. Comput. Syst.* 124 1–9

Afroosa M, Rohith B, Paul A, Durand F, Bourdallé-Badie R, Sreedevi P V, De Viron O, Ballu V and Shenoi S S C 2021 Madden-Julian oscillation winds excite an intraseasonal see-saw of ocean mass that affects Earth's polar motion Commun. Earth Environ. 2 139

Baduru B, Paul B, Banerjee D S, Sanikommu S and Paul A 2019
Ensemble based regional ocean data assimilation system for the Indian Ocean: implementation and evaluation *Ocean Modelling* 143 101470

Balogun A L and Adebisi N 2021 Sea level prediction using ARIMA, SVR and LSTM neural network: assessing the impact of ensemble ocean-atmospheric processes on models' accuracy Geomatics Nat. Hazards Risk 12 653–74

Bonjean F and Lagerloef G S E 2002 Diagnostic model and analysis of the surface currents in the tropical pacific ocean *J. Phys. Oceanogr.* **32** 2938–54

Castillo-Trujillo A C, Kwon Y O, Fratantoni P, Chen K, Seo H, Alexander M A and Saba V S 2023 An evaluation of eight

- global ocean reanalyses for the Northeast US continental shelf *Prog. Oceanogr.* **219** 103126
- Chapman J W, Klaassen R H G, Drake V A, Fossette S, Hays G C, Metcalfe J D, Reynolds A M, Reynolds D R and Alerstam T 2011 Animal orientation strategies for movement in flows Curr. Biol. 21 R861–70
- Chen H, Lu T, Huang J, He X and Sun X 2023 An improved VMD–EEMD–LSTM time series hybrid prediction model for sea surface height derived from satellite altimetry data *J. Mar. Sci. Eng.* 11 2386
- Dean J and Monga R 2015 TensorFlow: Large-scale machine learning on heterogeneous distributed systems (arXiv:1603.04467)
- Dohan K 2021 Ocean surface current analyses real-time (OSCAR) surface currents—final 0.25 degree (version 2.0) (PO.DAAC) (https://doi.org/10.5067/OSCAR-25F20)
- Federico I, Pinardi N, Coppini G, Oddo P, Lecci R and Mossa M 2017 Coastal ocean forecasting with an unstructured grid model in the southern Adriatic and northern Ionian seas Nat. Hazards Earth Syst. Sci. 17 45–59
- Fix E and Hodges J L 1952 Discriminatory analysis: nonparametric discrimination: small sample performance (available at: https://apps.dtic.mil/sti/pdfs/ADA800391.pdf)
- Francis P A, Jithin A K, Effy J B, Chatterjee A, Chakraborty K, Paul A and Satyanarayana B V 2020 High-resolution operational ocean forecast and reanalysis system for the Indian ocean *Bull. Am. Meteorol. Soc.* **101** E1340–56
- Garçon V C, Oschlies A, Doney S C, McGillicuddy D and Waniek J 2001 The role of mesoscale variability on plankton dynamics in the North Atlantic *Deep Sea Res. II* 48 2199–226
- Gill A E 2016 Atmosphere—Ocean Dynamics (Elsevier)
 Guillou N and Chapalain G 2021 Machine learning methods
 applied to sea level predictions in the upper part of a tidal
- estuary *Oceanologia* 63 531–44
 Hewamalage H, Bergmeir C and Bandara K 2021 Recurrent neural networks for time series forecasting: current status and future directions *Int. J. Forecasting* 37 388–427
- Hochreiter S and Schmidhuber J 1997 Long short-term memory Neural Comput. 9 1735–80
- Huang N E, Shen Z, Long S R, Wu M C, Shih H H, Zheng Q, Yen N-C, Tung C C and Liu H H 1998 The empirical mode decomposition and the Hilbert spectrum for nonlinear and non-stationary time series analysis *Proc. R. Soc. A* 454 903–95
- Jörges C, Berkenbrink C and Stumpe B 2021 Prediction and reconstruction of ocean wave heights based on bathymetric data using LSTM neural networks *Ocean Eng.* 232 109046
- Kartal E and Altunkaynak A 2024 Empirical-singular-wavelet based machine learning models for sea level forecasting in the bosphorus strait: a performance analysis *Ocean Modelling* 188 102324
- Kullback S and Leibler R A 1951 On information and sufficiency Ann. Math. Stat. 22 79–86
- Lellouche J M, Bourdalle-Badie R, Greiner E, Garric G, Melet A, Bricaud C and Drevillon M 2021 The Copernicus global 1/12° oceanic and sea ice reanalysis *EGU General Assembly Conf. Abstracts* pp EGU21–14961
- Lou R, Lv Z, Dang S, Su T and Li X 2023 Application of machine learning in ocean data Multimedia Syst. 29 1815–24

- Murphy A H 1993 What is a good forecast? An essay on the nature of goodness in weather forecasting *Weather Forecasting* **8** 281–93
- Nikoo M R, Kerachian R and Alizadeh M R 2018 A fuzzy KNN-based model for significant wave height prediction in large lakes *Oceanologia* **60** 153–68
- Pedlosky J 2013 *Geophysical Fluid Dynamics* (Springer)
 Pölz A, Blaschke A P, Komma J, Farnleitner A H and Derx J 2024
 Transformer versus LSTM: a comparison of deep learning
 models for karst spring discharge forecasting *Water Resour*.
- Prasad V S, Mohandas S, Dutta S K, Gupta M D, Iyengar G R, Rajagopal E N and Basu S 2014 Improvements in medium range weather forecasting system of India *J. Earth Syst. Sci.* 123 247–58

Res. 60 e2022WR032602

- Qin Y, Su C, Chu D, Zhang J and Song J 2023 A review of application of machine learning in storm surge problems J. Mar. Sci. Eng. 11 1729
- Rohith B, Paul A, Durand F, Testut L, Prerna S, Afroosa M, Ramakrishna S S V S and Shenoi S S C 2019 Basin-wide sea level coherency in the tropical Indian Ocean driven by Madden–Julian Oscillation *Nat. Commun.* **10** 1257
- Shola A A, Huaming Y U and Kejian W U 2024 Review of Machine Learning Methods for Sea Level Change Modeling and Prediction (Science of The Total Environment) p 176410
- Sudre J, Maes C and Garçon V 2013 On the global estimates of geostrophic and Ekman surface currents *Limnol. Oceanogr.* 3 1–20
- Thomas C S, Howie C A and Smith L S 2005 A new singly connected network classifier based on mutual information *Intell. Data Anal.* 9 189–205
- Tur R, Tas E, Haghighi A T and Mehr A D 2021 Sea level prediction using machine learning *Water* 13 3566
- Umgiesser G, Canu D M, Cucco A and Solidoro C 2004 A finite element model for the Venice Lagoon. Development, set up, calibration and validation J. Mar. Syst. 51 123–45
- Venkatesan R, Shamji V R, Latha G, Mathew S, Rao R R, Muthiah A and Atmanand M A 2013 *In situ* ocean subsurface time-series measurements from OMNI buoy network in the Bay of Bengal *Curr. Sci.* **104** 1166–77 (available at: www.jstor.org/stable/24092396)
- Winona A Y and Adytia D 2020 Short term forecasting of sea level by using 1stm with limited historical data 2020 Int. Conf. on Data Science and Its Applications (Icodsa) (IEEE) pp 1–5
- Witten I H, Frank E, Hall M A, Pal C J and Data M 2005 Practical machine learning tools and techniques *Data Mining* vol 2 (Elsevier) pp 403–13
- Yavuzdoğan A and Kayıkçı E T 2025 Advancing sea level anomaly modeling in the black sea with LSTM auto-encoders: a novel approach *Ocean Modelling*
- Zhang S, Zhao Z, Wu J, Jin Y, Jeng D-S, Li S, Li G and Ding D 2024 Solving the temporal lags in local significant wave height prediction with a new VMD-LSTM model *Ocean Eng.* 313 119385
- Žust L, Fettich A, Kristan M and Ličer M 2021 HIDRA 1.0: deep-learning-based ensemble sea level forecasting in the northern Adriatic Geosci. Model Dev. 14 2057–74